



Geotechnical Horizons: Innovations & Challenges

15 – 18 October 2025 • Auckland, New Zealand

Inertia and Kinematic Soil-structure Interaction Foundation Design in Response to Seismic Events

Y.Y. Tay

EDG Consulting Pty. Ltd., Australia.

G. Carnero, A. Beall & R. E. May

WSP Australia Pty. Ltd., Australia.

ABSTRACT

In the field of earthquake engineering, structural response studies address the inertial loading of the superstructure that results in tower lateral, rotational and torsional movements. The swaying of a tower causes its pile foundations to move, where structural forces are transferred to the top of the piles. As a first approximation, the lateral loads of the tower are resisted by the upper portions of the piles, and overturning moments resisted by push–pull pile actions. In addition to inertia loading, kinematic loading due to seismic shear waves travelling up through a soil column from bedrock causes soil to move against piles, therefore generating additional pile lateral loads and moments along the pile lengths. This paper presents an approach undertaken for inertia and kinematic soil-structure interaction assessments of a tower in a seismic-sensitive area in the Pacific. The project site geology is complex, comprising rock formation that had been subjected to tectonic deformation, causing intense folding, faulting and the rock head dipping steeply by nearly 30 m over the tower footprint. As a result, 3-dimensional numerical modelling has been adopted for inertia soil-structure interaction assessment. For kinematic soil-pile interaction assessment, free-field movements were assessed one-dimensionally and then superimposed onto pile foundations based on pseudo-static analysis for the determination of pile actions. Pile actions from both inertia and kinematic loading were then combined for design.

1 INTRODUCTION

This paper discusses the approach we have undertaken for the seismic foundation design of a tower located at the northern margin of the Australian tectonic plate which is seismic-sensitive. The tectonic complexity of the region results from the Pacific and Caroline Sea tectonic plates to the north obliquely converging with the Australian plate to the south. The complex boundary zone between the Australian, Pacific, and Caroline Sea plates comprises a series of seismically active subduction zones, small microplates, and major crustal faults that accommodate plate boundary deformation. This ongoing crustal deformation generates many earthquakes, including several large-magnitude ($>$ moment magnitude M7) historical earthquakes. In this context, the site geology is complex with a rock formation that had been subjected to tectonic deformation and the top of the rock head dipping about 30 m across the tower footprint.

The tower foundation comprised small perimeter pile groups (1 to 4 no. piles in each group) with individual pile caps supporting isolated structural columns, and a large pile group of approximately 100 no. piles with a raft supporting the tower core. The pile caps are connected by a base slab suspended over residual soils in the west and highly weathered rock in the east. The raft is located 6 m below the surrounding piles on residual soils. The pile toes were terminated at six different levels due to the varying rock head levels.

2 GROUND CONDITIONS AND SEISMIC SITE CLASS

The main geologic unit underlying the tower site comprises a sequence of fine grained calcarenite beds and siliceous argillite beds. It has been subjected to tectonic deformation, causing relatively intense folding, faulting and low-level metamorphism. Structural measurements in the area show a general trend of bedding dipping 30 m across the tower footprint with different strikes and dips. The rock mass has been subject to weathering to a significant depth, and residual soils can be several metres thick. The subsurface conditions at the site comprise fill overlying, residual soil, and Siltstone bedrock of varying weathering stages.

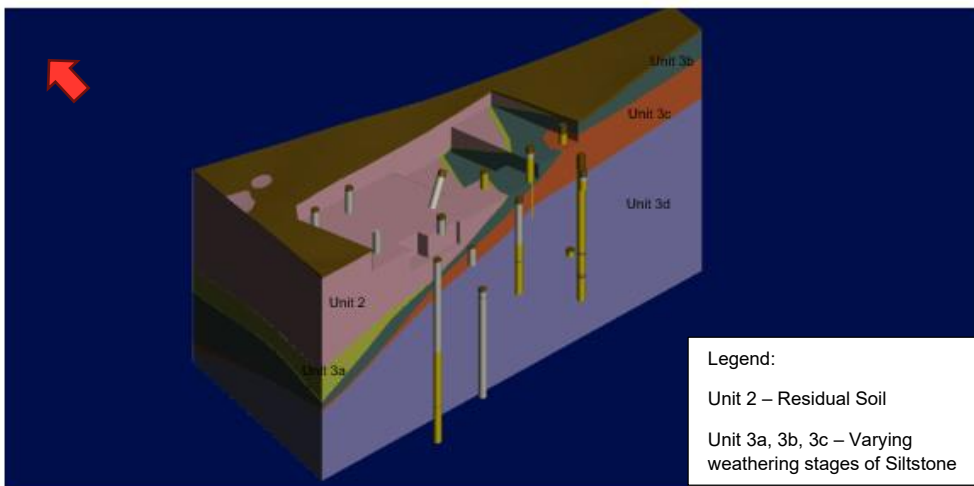


Figure 1: 3D Geological Model

Site investigation, including in-situ field testing, laboratory testing and bi-directional pile load testing, had been conducted to determine geotechnical parameters for foundation design.

The averaged shear wave velocity (V_s) of the upper 30 m below ground surface (V_{S30}) is about 250 m/s (Figure 2) based on downhole vertical seismic profiling measurements from boreholes drilled in Profile 1 site (i.e. 14m thick residual soil) and is more than 400 m/s based on boreholes drilled near Profile 2 site (i.e. no residual soil). These V_{S30} values correspond with ASCE Standard 7-16 (2017) site classifications of soil Site Class D and soil Site Class C for Profile 1 (deep soil) and Profile 2 (shallow rock) locations, respectively.

Two analytical models were developed for the seismic ground response studies. Model V_S Profile 1 and Profile 2 were designed to obtain similar values of site-specific V_{S30} and terminate upon achieving a seismic engineering bedrock of 760 m/s. Due to the relatively deep weathered bedrock at Profile 1 location, V_S measurements did not achieve 760 m/s upon completion of the in-situ tests. To extend the Profile 1 model, an averaged V_S profile from Profile 2 was applied at the interface between residual soil and bedrock. A V_S profile was interpolated for Profile 3 (intermediate between Profiles 1 and 2), as shown in Figure 3, by adopting a similar profile as Profile 1 (both relatively deep soil profiles) from the ground surface to a representative soil-rock interface, while adopting a V_S gradient with depth through rock that mirrors Profiles 1 and 2.

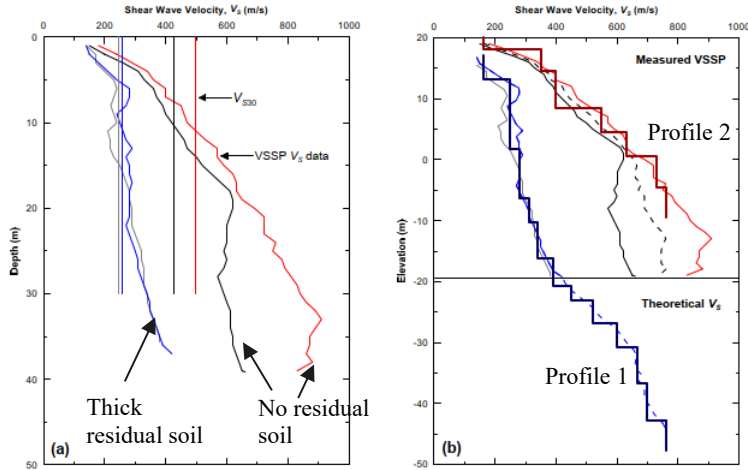


Figure 2: (a) Downhole Vertical Seismic S-wave Profiles and (b) SGRA Model Profiles

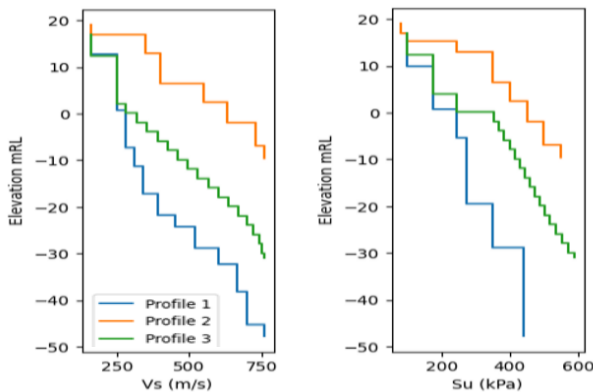


Figure 3: Assumed shear wave (V_S) and undrained shear strength (S_u) profiles for the DEEPSOIL profiles

3 SEISMIC FOUNDATION DESIGN

3.1 Approach

Seismic foundation design considers pile actions resulting from kinematic effects induced by ground movement and inertia effects induced by the swaying of the structure during an earthquake. The approach undertaken for seismic foundation design in this study included the following steps:

- Carry out site specific seismic hazard site assessment based on earthquake time histories and shear wave velocities,
- Determine free field response from seismic ground response analysis using the software DEEPSOIL (v7), noting that there is no potential for liquefaction and lateral spread at the site.

- Carry out kinematic soil-pile interaction (pseudo-static) assessment by superimposing the peak soil movement onto the pile using software LPILE (v2022.12.07) to determine kinematic pile actions,
- Undertake inertia soil-structure interaction adopting structural forces based on structural spectra responses amongst other loading sources in software PLAXIS 3D (V21) to determine inertial pile actions,
- Combine pile actions resulting from kinematic and inertia effects.

The following sections detail each assessment undertaken.

3.2 Free Field Response from Seismic Ground Response Analysis

We undertook a one-dimensional (1D) seismic ground response analysis (SGRA) for the site using the software DEEPSOIL, effectively assuming horizontally homogeneous soil layers, to calculate the free field response. Variability in the seismic velocity profile across the site was incorporated by separately modelling three soil profiles, representative of the contrasting depths to rock - Profile 1 (deep soil), Profile 2 (shallow rock) and Profile 3 (intermediate between profiles 1 and 2). This approach does not account for three-dimensional effects such as wave scattering by the inclined rock and soil layers (Stewart et al., 2014). Validation of 1D and 2D site response models against measurements from vertical arrays indicate that 1D models tend to over-estimate ground motion amplification (de La Torre et al., 2022) and we therefore consider our approach to be conservative. The benefits of 1D modelling using DEEPSOIL are that it accurately models non-linear soil hysteresis (i.e. without requiring the equivalent-linear approximation) and includes standard practice modulus reduction and damping models (e.g. Darendeli, 2001), non-masing loading/unloading and high-strain shear strength corrections, consistent with laboratory soil testing (Hashash et al. 2017). There were 11 two-component earthquake acceleration time histories developed for bedrock ground motion input. The rapid computation time of 1D models allowed for each profile to be re-calculated for every time history component. Conversely, setting up a PLAXIS model (either 2D or 3D) involves more complex calibration of constitutive modelling and boundary conditions, as well as prohibitive computation and analysis times for the input of many input time histories. We modelled non-linear damping of ground motion using the Darendeli (2001) soil damping model with parameters inferred from V_s and assumed shear strength shown in Figure 3. Spectral acceleration is a key output of SGRA and is shown in Figure 4.

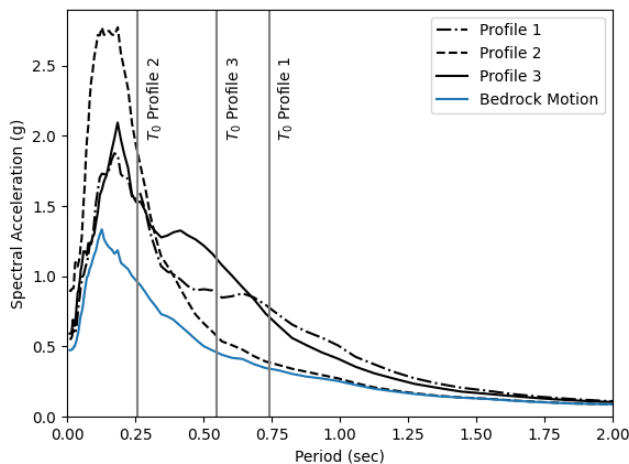


Figure 4: Mean spectral acceleration for Profiles 1, 2 and 3, compared to the mean bedrock motion

The earthquake bedrock ground motions used in the SGRA were developed by undertaking a Probabilistic Seismic Hazard Analysis and Earthquake Acceleration Time History Development specific to the site ground conditions at 1/2,475 Annual Exceedance Probability. The V_s profile controls the amplification of earthquake

ground motions. The fundamental period of Profile 3 is calculated as 0.55 s, compared to the periods of 0.74 s and 0.26 s calculated for Profiles 1 and 2, respectively.

The mean surface spectral acceleration for Profiles 1, 2 and 3 is compared to the mean input bedrock motion. The highest spectral acceleration occurs over approximately 0.1-0.3 s for each profile, which is related to a similar period range of high spectral acceleration in bedrock motion. Profile 2 has the highest spectral acceleration at this period range due to its short fundamental period. Profiles 1 and 3 have amplified spectral accelerations at periods approximately corresponding to their longer fundamental periods. The spectral accelerations calculated for Profile 3 are similar to Profile 1, as both have a thick residual soil layer. However, the spectral acceleration of Profile 3 is higher than Profile 1 over periods 0.3-0.6 s near the Profile 3 fundamental period.

The maximum free field soil displacement is required to model lateral soil loading on the piles and was calculated using DEEPSOIL for each profile (Figure 5). The relative soil displacement reached more than 20 mm for Profile 1, and the maximum shear strain was <1% for all profiles. The maximum displacement is higher for Profiles 1 and 3, related to the relatively low V_s and shear strength of the residual soil layer. The maximum displacement does not have a sharp gradient at the soil-rock interface, as the assumed V_s profiles do not have a significant step increase at the soil-rock interface (Figure 3).

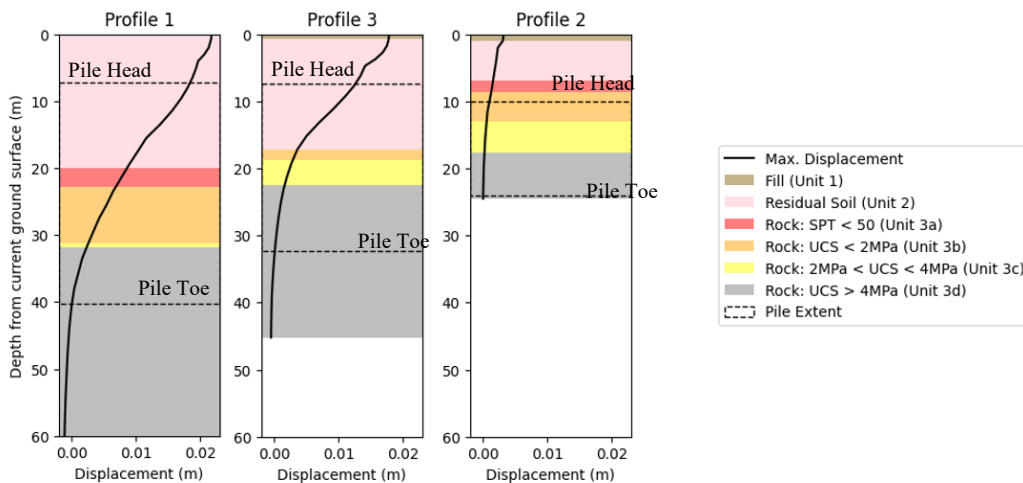


Figure 5: Maximum free field soil displacement

3.3 Kinematic Soil-Pile Interaction Assessment

Soil-pile interaction was considered for Profiles 1, 2 and 3. Piles were modelled as elastic, incorporating a 0.3 times reduction factor of the rigidity (EI) to reflect the assumed cracked condition. The maximum free field relative soil displacement between pile toe level and pile head is <1 mm for Profile 2 and is considered to produce negligible kinematic soil-pile interaction. Kinematic soil-pile interaction was therefore only modelled for Profiles 1 and 3.

Soil-pile interaction is modelled with LPile using Beam on Nonlinear Winkler Foundation analysis, incorporating p-y load-displacement springs using the Stiff Clay (Reese et. al 1975) and Massive Rock (Liang et. al 2009) formulations included within LPile for the residual soil and rock layers respectively. Rock was further divided into the layers shown in Figure 4. Secant moduli of the generated p-y curves of each layer were calculated and compared with the stiffnesses of the residual soils and rock layers to check suitability of formulations adopted for the soil-pile interaction assessment. The pile head is assumed to be fixed with zero rotation. The LPile results for Profiles 1 and 3 are shown in Figures 6 and 7, respectively, and summarised in Table 1. The pile deflection is the same as the soil movement within the residual soil layer;

however, at the soil-rock interaction level, the pile deflection is smaller than the soil movement with a discernible pile bending curvature; noting that the same soil and pile movements are not anticipated as soils deform in shear and piles deform in bending. The highest modelled bending moments occurred in the two profiles immediately below the soil-rock interface, related to both the change in free field displacement close to the interface and the change in stiffness between the soil and rock p-y properties. The bending moments at the pile head are lower than that at the soil-rock interface due to kinematic effects and are approximately 25% of the pile moment capacity.

Table 1: Maximum soil displacement bending moment and shear force calculated with LPile

| Profile | Residual Soil Thickness (m) | Max. Soil Displacement (mm) | Max. Bending moment* (kNm) | Resultant BM** | Max. Shear Force (kN)* | Resultant SF** | Location of Max. Pile Actions |
|---------|-----------------------------|-----------------------------|----------------------------|----------------|------------------------|----------------|------------------------------------|
| 1 | 14 | 18 | 160 400 | 170 420 | 0 520 | 0 540 | Top of rock Soil-rock interface |
| 3 | 12 | 13 | 210 300 | 220 310 | 0 370 | 0 390 | Top of rock Soil-rock interface |

* Forces in the x-direction. The same actions are assumed for the y-direction.

**Resultant is calculated using 100% major direction action and 30% minor direction action based on ASCE 7-16 commentary.

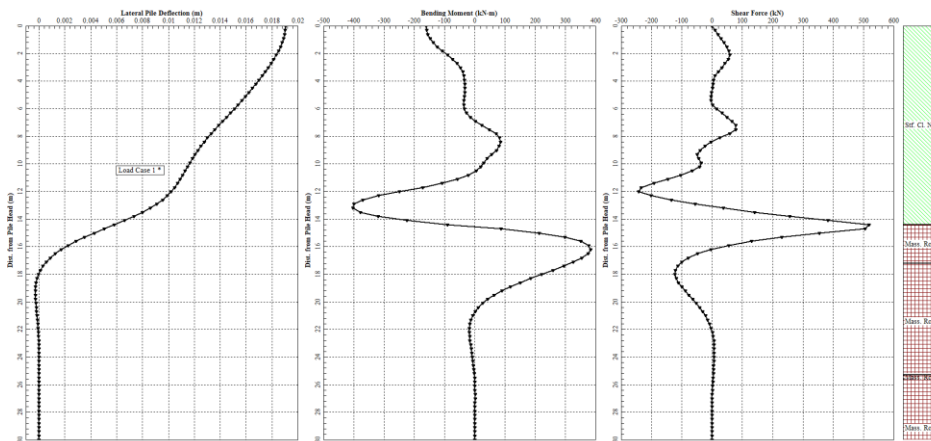


Figure 6: Profile 1 pile deflection, bending moment and shear force calculated using LPile

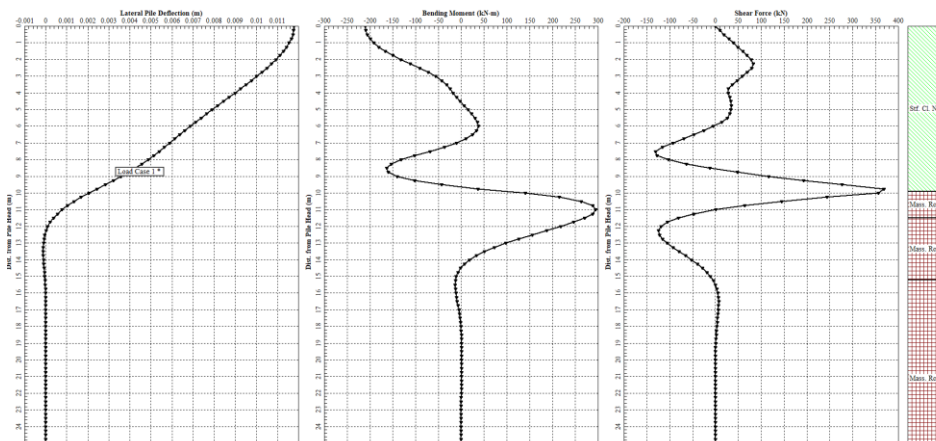


Figure 7: Profile 3 pile deflection, bending moment and shear force calculated using LPile

3.4 Inertia Soil-Structure Interaction Assessment

We undertook an inertia soil-structure interaction assessment using PLAXIS 3D due to the complexity of the site geology where rock units dip 30 m across the tower footprint. Piles were modelled as embedded beam elements with an assumed cracked-section stiffness ($0.7 EI$) and the pile caps/ raft were modelled as plates with strength-reduction interface elements. Mohr–Coulomb constitutive modelling was adopted as lateral pile movements was less than 10 mm (i.e., within elastic range). Small strain stiffness was considered for transient load case.

Vertical and horizontal structural loads were applied to the model to calculate pile head deflections and stiffnesses. Iteration between structural and geotechnical models was undertaken such that convergence of pile forces and deflection in the models was achieved. The results of maximum vertical and horizontal pile reactions for the 3 profiles are presented in Table 2. The maximum bending moments due to inertia loading occurs at pile head and is zero at soil-rock interface.

Table 2: Maximum bending moment and shear force calculated with PLAXIS 3D due to inertia loading

| Profile | Residual Soil Thickness (m) | Max. Axial Compression (kN) | Max. Axial Tension (kN) | Max. Bending moment* (kNm) | Max. Shear Force* (kN) | Location of Max. Pile Actions |
|---------|-----------------------------|-----------------------------|-------------------------|----------------------------|------------------------|------------------------------------|
| 1 | 14 to 18 | 7010 | 0 | 1700 0 | 1100 0 | Top of pile Soil-rock interface |
| 2 | 0 to 2 | 7910 | -130 | 1600 0 | 1500 0 | Top of pile Soil-rock interface |
| 3 | 5 to 13 | 7510 | -2100 | 1400 0 | 1000 0 | Top of pile Soil-rock interface |

* Resultant is calculated using 100% major direction action and 30% minor direction action based on ASCE 7-16 commentary.

Static loading in the vertical direction typically resulted in high pile loads at the edges of the rigid raft at the tower core, which generated a relatively uniform settlement. Push-pull loading translated from the swaying of the tower as seismic response resulted in maximum and minimum pile loads near the edges of the raft and tower.

In the horizontal direction, larger pile shear and moments were in the direction upslope of the rock head compared to actions downslope. The maximum actions occurred near the top of each pile as fixity in the rotational direction was considered in the assessment. At the soil-rock interface there were residual pile actions in some of the piles. Large pile shear and moment typically occurred along the edges and corners of the tower core and the tower as shown in Figure 8. The smaller pile shear and moment at the centre of a pile group are due to shadowing effects and pile group interaction (hence “softer” centre piles). Additionally, the piles are mainly located at three different levels therefore shadowing effects of walls were also observed.

3.5 Combined Pile Actions

Pile shears and moments due to inertia and kinematic loading were combined for the foundation design. As the natural period of the superstructure is greater than that of the ground, the maximum pile shear and moments were taken to be the square root of the sum of the squares of the moments due to each effect (Tokimatsu et. al. 2005). Pile shear and moments due to inertia loading occurred near the top of the pile, with residual shear along the pile. Pile shear and moments due to kinematic loading were greater near the soil-rock interface than at the pile head. Maximum combined pile actions at the pile head and soil-rock interface are presented in Table 3.

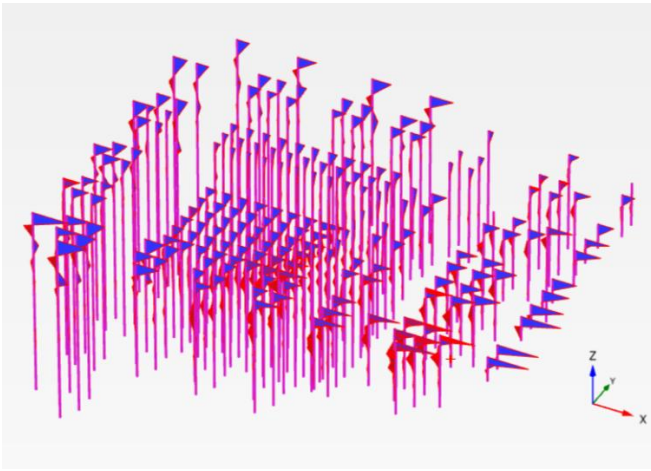


Figure 8: Pile bending moment distribution (x-direction) upslope of rock-head

The results showed that additional bending moment and shear force at soil-rock interface when considering the combined loading of kinematic and inertia effects even though there are no sharp differences between stiffnesses of residual soil and rock based on the V_s profile. Therefore, sufficient reinforcement extending to below the depth of the soil-rock interface is required.

Table 3: Maximum bending moment and shear force calculated with PLAXIS 3D due to combined loading

| Profile | Residual Soil Thickness (m) | Max. Bending Moment* (kNm) | Max. Shear Force* (kN) | Location of Max. Pile Actions |
|---------|-----------------------------|----------------------------|------------------------|------------------------------------|
| 1 | 14 | 1700 420 | 1100 540 | Top of pile Soil-rock interface |
| 2 | 0 | 1600 0 | 1500 0 | Top of pile Soil-rock interface |
| 3 | 10 | 1400 310 | 1000 390 | Top of pile Soil-rock interface |

* Resultant is calculated using 100% major direction action and 30% minor direction action based on ASCE 7-16 commentary.

4 SUMMARY

Site specific seismic hazard assessment and seismic ground response analysis (SGRA) were undertaken given the lateral variability of the ground strata where the rock head dips 30 m across the tower footprint.

For seismic foundation design, free field soil displacement due to kinematic effects of earthquake was calculated from SGRA for three soil profiles representative of the contrasting residual soil depths to rock. Following this, a kinematic soil-pile interaction (pseudo-static) assessment was carried out by imposing the predicted free field soil movement onto the piles to determine pile actions. Additionally, inertia soil-structure interaction assessment was carried out using geotechnical numerical 3D modelling based on structural forces from inertia effects (structural spectral responses), amongst other load combinations. Maximum pile shear and moment from kinematic loading occurred near the soil-rock interface, and the actions occurred near the pile head from inertia loading. As the natural period of the superstructure is greater than that of the ground, the pile actions due to inertia and kinematic effects were combined based on the square root of the sum of the squares of the actions due to each effect. The max bending moment and shear force of the combined loading appear to be at pile head with smaller but still significant values at soil-rock interface level.

The above approach for this rather complex seismic foundation design was adequately detailed to capture the foundation loading demands and was conducted over a reasonable timeframe for the project. A fully dynamic time-domain assessment as an alternative to a pseudo-static assessment is more time consuming but may be considered for comparison in future studies.

5 REFERENCES

- ASCE Standard 7-16. (2017). Minimum design loads and associated criteria for buildings and other structures.
- Darendeli, M. B. (2001). Development of a new family of normalised modulus reduction and material damping curves. The University of Texas at Austin.
- De la Torre, C. A., EERI, M., Bradley, B.A., Stewart J.P., McGann, C.R. (2022). Can modelling soil heterogeneity in 2D site response analyses improve predictions at vertical array sites? *Earthquake Spectra*, Vol. 38 (4) 2451-2478.
- Hashash, Y.M.A., Musgrove, M.I., Harmon, J.A., Ilhan, O., Groholski, D.R., Philips, C.A., Park, D. (2017). DEEPSOIL v7.0, User Manual.
- Liang, R., Yang, K., & Nusairat, J. (2009). P-y criterion for rock mass. *Journal of geotechnical and geoenvironmental engineering*, 135(1), 26-36.
- Reese, L. C., Cox, W. R., & Koop, F. D. (1975). Field testing and analysis of laterally loaded piles on stiff clay. Offshore technology conference (pp. OTC-2312). OTC.
- Stewart, J. P., et al. (2014). Site effects in geotechnical earthquake engineering. *Earthquake Geotechnical Engineering Design*.
- Tokimatsu, K., Suzuki, H. and Sato, M. (2005), Effects of inertial and kinematic interaction on seismic behaviour of pile with embedded foundation, *Soil Dynamics and Earthquake Engineering* 25, 753-762.